5th US Combustion Meeting
Organized by the Western States Section of the Combustion Institute
and Hosted by the University of California at San Diego
March 25-28, 2007.

Experimental and Numerical Investigation of Strained Laminar Flame Speeds for $H_2/O_2/N_2$ Mixtures at Elevated Temperature

J. Natarajan, T. Lieuwen and J. Seitzman

School of Aerospace Engineering
Georgia Institute of Technology
Atlanta GA, 30332-0150

Laminar flame speeds and strain sensitivities of mixtures of H_2 and air, or air highly diluted with N_2 (O_2:N_2 1:9) have been measured for a range of equivalence ratios at high preheat conditions (~700K) using a nozzle generated, 1-D, laminar, wall stagnation flame. The measurements are compared with numerical predictions based on three detailed kinetic models (GRIMech 3.0, a H_2/CO mechanism from Davis *et al*. and a H_2 mechanism from Li *et al.*). Sensitivity of the measurements to uncertainties in boundary conditions, e.g., wall temperature and nozzle velocity profile (plug or potential) are investigated through detailed numerical simulations and shown to be small. The flame speeds and strain sensitivities predicted by the models are in reasonable agreement with the measurements for H_2 with standard air at very lean conditions. For H_2 with N_2 diluted air, however, all three mechanisms significantly over predict the measurements. The disagreement between experimental data and the predictions for the N_2 diluted flames also increases for leaner mixtures. In contrast, the models under predict flame speeds for H_2 with both standard and N_2 diluted air for room temperature reactants, based on comparisons with measurements in the literature. Thus, we find that the temperature dependence of the hydrogen flame speed as predicted by all the models is greater than the actual temperature dependence (for both standard and diluted air). Finally, the models are found to under predict the measured strain sensitivity of the flame speed for H_2 burning in N_2 diluted air, especially away from stoichiometric conditions.

1. Introduction

One of the most extensively studied kinetic mechanisms is that of hydrogen combustion, because of its relative simplicity and because of its importance in understanding combustion of hydrocarbon fuels in general. Hydrogen is also an interesting fuel from a practical standpoint, due to its intense burning characteristics and because of its potential to reduce greenhouse gas emissions. For example, recent interest has been focused on synthetic fuel gas (syngas) combustion. Syngas is derived from coal through a gasification process, and it is a promising fuel source for low emission and high efficiency power generation. It is mainly composed of H_2, CO, N_2 and CO_2 in varying amounts, with typically lower levels of H_2O, CH_4, and other higher order hydrocarbons.[1,2] Extensive research has been conducted to understand the fundamental combustion properties of these fuel mixtures. These include experimental determination of laminar flame speed, ignition delay and flame structure. Laminar flame speed is an important parameter of a combustible mixture as it contains fundamental information regarding reactivity, diffusivity, and exothermicity.

Several prior studies have included measurements of the flame speeds of syngas mixtures.[3-5] For example, stretch corrected laminar flame speed measurements with counter-flow flames[6] and spherically expanding flames[7-10] have been obtained. Various reaction mechanisms have been proposed for the H_2/CO combustion based on these measurements.[11, 12] Since most of the flame speed measurements were obtained for stoichiometric and fuel-rich mixtures, and with room temperature reactants, the applicability of the proposed kinetic models to low emissions, lean premixed gas turbine combustion is uncertain. Recently, the laminar flame speeds of H_2/CO mixtures have been measured over a range of preheat temperature (up to 700 K) and fuel composition.[13] The results indicated that for medium and high H_2 content fuel mixtures, the models studied over predict the measured flame speeds at high preheat temperature and lean conditions. Hence it is important to investigate the effect of preheat on flame speeds of pure H_2 fuels at lean conditions. As applications involving H_2 combustion can also entail significant levels of diluent gases (e.g., syngas combustion), we also consider laminar flame speeds for reactant mixtures with high amounts of N_2 dilution.

Thus, the primary objective of the present study is to measure laminar flame speed and its sensitivity to strain for $H_2/O_2/N_2$ fuel mixtures at high preheat temperature (700 K) and under lean conditions. A stagnation flame technique is employed in this work. To ascertain the accuracy of current models, the measurements are compared with the predictions of leading chemical kinetic mechanisms in order to validate them at the high preheat temperatures found in gas turbine combustors.

2. Experimental Facility and Measurement Method

Strained laminar flame data were acquired in a stagnation flow configuration. This configuration, like the more common opposed (jet) flow approach,[14] allows for stretch-corrected flame speed measurements of a one-dimensional laminar flame. Furthermore, it is advantageous over the opposed flow arrangement for determining laminar flame speeds for the following reasons: (1) the use of a solid wall leads to more stable flames, (2) problems related to heating of the upper burner are eliminated, and (3) ease of operation of a single jet.

A general schematic of the stagnation flow burner is shown in Figure 1. The reactants (H_2, O_2, and N_2) flow rates are monitored with rotameters, and they are premixed in the mixing section ahead of the burner. All the rotameters are calibrated with a bubble flow meter and wet test meter to better than ± 1% accuracy, with fuel and air flows in the range of 0.1 to 50 slpm. The desired flow rate of the premixed fuel mixture is sent to the burner while the remainder is bypassed. With this arrangement, the average velocity of the mixture at the exit of the burner is easily adjusted without altering the equivalence ratio. The burner is formed from a smoothly contoured nozzle with high contraction ratio, in order to create a uniform velocity profile at the burner exit and a uniform flame stretch throughout the flame area. Moreover, the high contraction ratio contoured nozzle ensures laminar flow even at high Reynolds number based on the burner exit diameter.

Two nozzles with exit diameters (D=6.25 and 9 mm) are employed to produce a stable flame, with higher flame speed mixtures requiring the smaller nozzle. Flow straighteners placed upstream of the contoured nozzle reduce any unsteadiness in the incoming flow. The exiting fuel/air mixture is surrounded by a N_2 coflow. Flow stagnation is achieved with a plug produced from a stainless steel rod (38 mm diameter). The end of the rod is first formed into a hemisphere

and then machined to produce a flat surface with 12.5 mm diameter. The rounded plug, compared to a flat plate, greatly improves flame stability especially at high flame speed conditions (e.g., high preheating). The distance (L) between the burner exit and stagnation plug is adjusted depending on the burning velocity. For high burning velocities, a lower L/D leads to a stable stagnation flame. In the current measurements, L/D ranges from 0.5 to 1. These L/D values are sufficiently large that the effect of finite domain on the measured flame speed can be considered small.[15] The use of a solid wall as a stagnation plane, as opposed to the counterflow configuration with adiabatic twin flames, is generally considered to have an insignificant effect on the measured unburned flame speed, provided that the flame is stabilized sufficiently away from the stagnation plane.[16] In all our experiments, the flame is located at least two flame thicknesses away from the plate (and generally more than 5 flame thicknesses). The effects of the solid wall are mainly downstream heat loss from the flame products to the wall and zero radial velocity gradient at the wall. A detailed numerical analysis of the influence of these effects on the unburned strained flame speed is reported in the Appendix for a typical fuel mixture and test condition considered here.

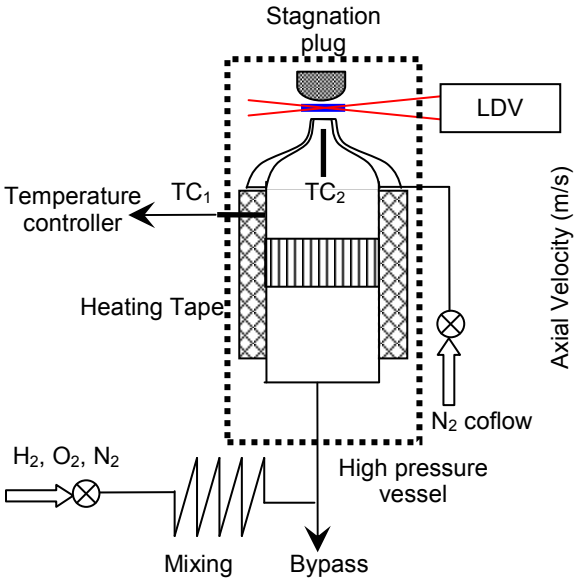

Figure 1. Schematic of the experimental setup (TC=thermocouple).

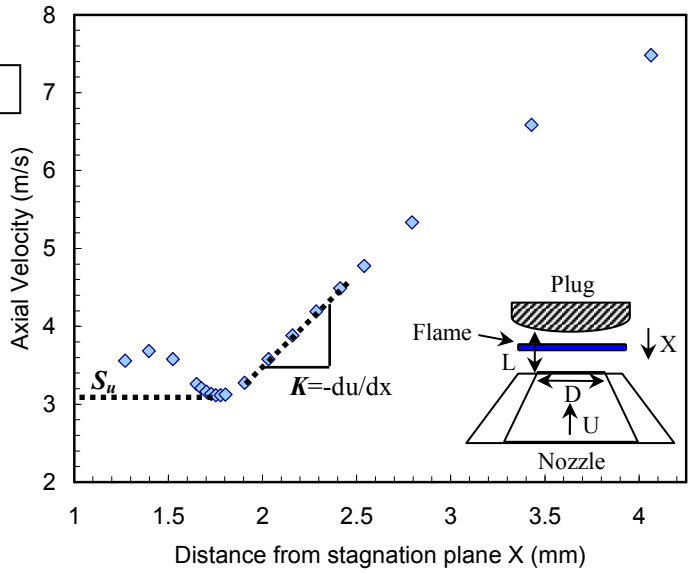

Figure 2. Measured axial velocity along the stagnation streamline for H_2 with N_2 diluted air (O_2:N_2 1:9) mixture at Φ=0.8 and 700 K preheat temperature (D = 9 mm; L = 6 mm).

The reactants are preheated by electrical resistance tape wrapped around the burner. Once the desired reactant temperature is achieved (as determined by a type-K thermocouple, TC_2, placed at the center of the burner 25 mm below the exit), the surface temperature of the burner is monitored by a second thermocouple, TC_1, and held constant by a temperature controller. The mixture temperature at the exit of the burner has a nearly uniform radial profile ($\Delta T \approx 3$-5 K). The axial velocity along the stagnation streamline is measured using a Laser Doppler Velocimetry (LDV) system. The fuel mixture is seeded with alumina (Al_2O_3) particles. The nominal size of these particles is chosen to be 1-2 μm in order to minimize thermophoretic effects.[17]

To illustrate this method, the measured axial velocity along the stagnation stream line for a typical stagnation flame is shown in Figure 2. The axial velocity decreases from the exit of the

nozzle and reaches a minimum where the preheat zone starts. After reaching a local minimum, the axial velocity increases sharply inside the flame and then decreases to zero at the wall. Based on a standard approach,[14] the minimum velocity before the preheat zone is considered as the reference strained unburned flame speed (S_u), and the maximum gradient of the axial velocity (as determined from the velocity measurements) ahead of the minimum velocity location is taken as the imposed strain rate (K) (see Figure 2). The imposed strain rate is controlled by changing the nozzle exit velocity. As the nozzle exit velocity increases, the strain rate increases, and the flame moves closer to the stagnation surface. For each fuel mixture, the strain rates and corresponding strained flame speeds are measured for a range of nozzle exit velocities. Effort has been taken to measure the strained flame speeds at as low strain rates as possible, limited either by flashback or flame stability (unsteadiness). The uncertainty in the strained flame speed measurement can be estimated from the rms fluctuation of the axial velocity at the location where the average velocity is a minimum. At each location along the stagnation stream line, 10,000 measurements were acquired and the rms fluctuations are 2-4% at the minimum velocity location for the conditions reported here.

3. Flame Speed Modeling

The experimental results are compared to predictions of a standard (Chemkin) one-dimensional flame model. The unstrained laminar flame speeds are calculated with the PREMIX algorithm, while the strained stagnation flames are simulated with OPPDIFF code. In the strained flame simulation, the distance between the nozzle and stagnation plane (L) was matched to the experimental value, since it can have a significant effect on the predicted strained flame speed. The plug flow boundary condition, which is a good representation of the measured nozzle data, is used at the nozzle exit. A detailed numerical analysis on the effect of nozzle exit boundary condition on the predicted flame speed is given in the Appendix. The predicted flame speed and strain rate are determined from the stagnation simulation with the same definitions that were applied to the experimental data (minimum velocity for flame speed and maximum preflame gradient for strain). In all the flame simulations, the converged solution was obtained for a large number of grid points by considering the gradient and curvature to be 0.1.

Three reaction mechanisms are employed in the simulations: GRI Mech 3.0,[18] a H_2/CO mechanism from Davis *et al*.[11] and a H_2 mechanism by Li *et al*.[19] The GRI mechanism has been tested and validated extensively for methane and natural gas combustion over a wide range of pressure and temperature conditions. It consists of 325 elementary chemical reactions with associated rate coefficients and thermochemical properties for the 53 species involved. The second, more recent mechanism was developed specifically for H_2/CO combustion. It consists of 14 species and 30 reactions, and incorporates recent updates for rate parameters and third body efficiencies of a few key reactions. It also includes modifications of thermodynamic and transport properties for species relevant to high temperature H_2 and CO oxidation. The third mechanism is an updated comprehensive kinetic model for hydrogen combustion. It consists of 19 elementary reactions and 11 species with associated rate coefficients and thermochemical properties. In all the simulations, multi-component diffusion and Soret effects (thermal diffusion) have been included, as they have significant influence on the calculated flame speeds.

4. Results and Discussion

As noted previously, the main objective of the present work is to validate the leading kinetic models for H_2 combustion by considering the effect of N_2 dilution and preheat temperature. Therefore, the laminar flame speed and strain sensitivity of $H_2/O_2/N_2$ mixtures were measured with the reactants initially at 700 K. The measurements are also compared with the predictions by all three kinetic models. To examine the temperature dependence of the flame speed, the predicted flame speeds at room temperature are also compared to literature values for experimental flame speed for the same mixtures.

Elevated reactant temperature results

H_2 with standard air

The strained flame speed for highly preheated H_2 air mixtures were measured for very lean conditions. The 6.25 mm diameter burner diameter was used with a stagnation surface spacing of L/D=0.8. The measured strained flame speed for various strain rates at Φ=0.3 and 0.5 are shown in Figure 3.

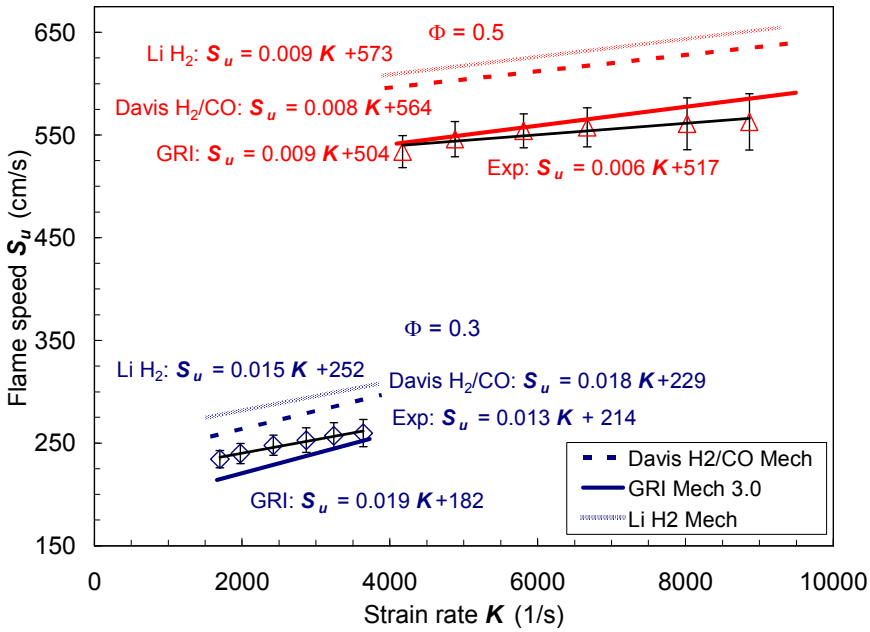

Figure 3. Strained laminar flame speeds for lean mixtures of H_2 at 700 K preheat temperatures; data (symbols and linear fit shown as thin line) and OPPDIF predictions (thick lines). Linear best-fits to the experimental data and the models are included as equations, with the first value being the strain sensitivity and the second value being the zero-strain extrapolated flame speed.

The measured flame speed increases linearly with the strain rate for both equivalence ratios, and the leaner case has the higher strain sensitivity. Figure 3 also shows the predicted strained flame speed from all three models for both equivalence ratios. For Φ=0.3, the H_2/CO and H_2 mechanisms over predict the measurements by 10% and 16%, respectively, for the investigated strain rate range, while the GRI mechanism predictions fall below measurements by about 6%. These discrepancies should be compared to the estimated uncertainties in the measurements and

modeling. As noted previously, the measurement precision was within ~3% for most of the measurements, as indicated by the error bars in Figure 3. As described in the Appendix, uncertainties in the boundary conditions between the experiments and the 1-d simulations could lower the model results by no more than ~2-3%. Thus the differences between the numerical and experimental results are larger than the estimated uncertainty. Yet the differences are not large (mostly within ±10-15%), so we conclude the model predictions are in good agreement with the measurements. Figure 3 also includes the equations for the linear best-fits to the measured and predicted flame speeds. The predicted strain sensitivities (slopes in the equations of Figure 3) from all the models are similar (0.0015-0.0019 cm), and they are in reasonable agreement with the measured strain sensitivity (0.0013 cm), though slightly higher (by 15-50%).

For Φ=0.5, the modeling results employing the GRI mechanism are now in excellent agreement with the measured strained flame speeds. As was seen with the leaner mixture, the H_2/CO and H_2 mechanisms over predict the measured flame speeds by 12% and 15%, respectively, about the same percentages as for Φ=0.3 case. The predicted strain sensitivities are even closer to one another in this case (0.008-0.009 cm) and are again somewhat higher (by 30-50%) than the measured strain sensitivity (0.006 cm).

Overall the agreement between the results and the predictions is good, with the GRI mechanism appearing to provide results that are in somewhat better agreement than the other two mechanisms. The flame speed results from the H_2 and H_2/CO mechanisms are quite close, though the H_2 mechanism tends to over predict the measured flame speeds slightly more.

H_2 with N_2 diluted air

In order to investigate the effect of dilution on highly preheated H_2 mixtures, experiments were conducted for pure H_2 fuel with highly N_2 diluted air (O_2:N_2 volume ratio of 1:9). The burner diameter used for this fuel mixture was 9 mm with an *L/D* of 0.66. Figure 4 shows the measured strained flame speeds at Φ=0.8 for a range of strain rates. The measured flame speed increases nonlinearly with the imposed strain rate, though the data appear closer to linear at low strain.

Also shown in Figure 4 are the predicted strain flame speeds in the same strain rate range as the measurements. Unlike the measurements, the predicted flame speeds increases linearly with strain rate. All three models over predict the measured flame speed. As in the undiluted cases, the GRI mechanism results are closest to the measurements and the H_2 mechanism produces the highest flame speeds. The GRI mechanism results are higher than the measurements by ~20% at lower strains, with the over prediction decreasing to 10% as strain increases. The H_2/CO and H_2 mechanism results are higher than the measurements by 30% and 35%, respectively, at low strain rates, with the discrepancy again decreasing at high strain.

Though the measured flame speeds increase nonlinearly with strain, we can estimate the strain sensitivity by a linear fit to the experimental results in the low strain region (1000-2000 s^{-1}) where the data are close to linear (see Figure 4). The strain sensitivities predicted by the models are again similar to one another (0.014-0.016 cm), but nearly three times lower than the measured sensitivity (0.049 cm). Thus if the results are extrapolated back to zero strain (to produce estimates of the unstrained flame speed), this leads to even larger discrepancies between the extrapolated model values (293-344 cm/s) and the extrapolated measurements (208 cm/s).

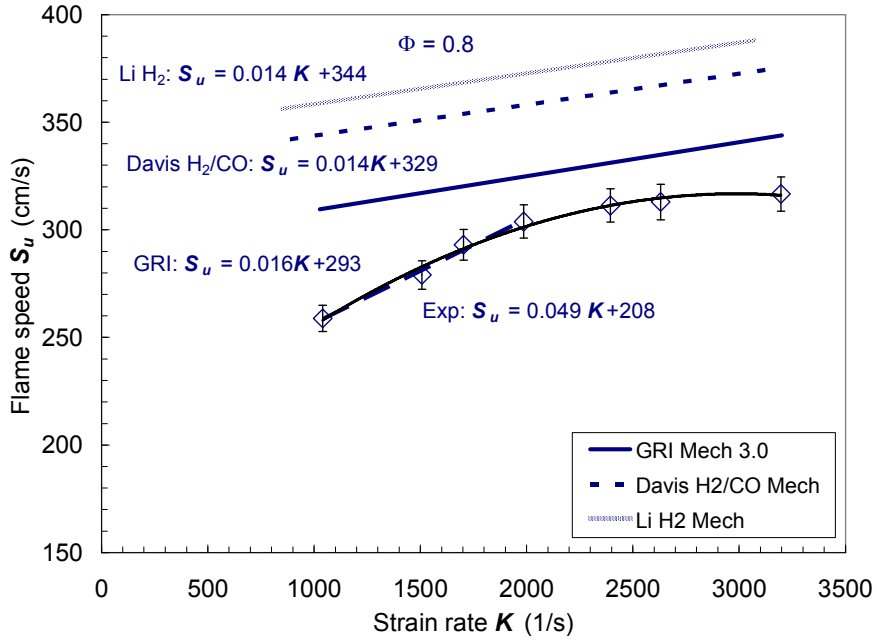

Figure 4. Strained laminar flame speeds for H_2 with N_2 diluted air (O_2:N_2 1:9) at 700 K preheat temperature; data (symbols and linear fit – thin line) and OPPDIF predictions (thick lines). Equations for best-fit lines to the experimental and model results are also shown.

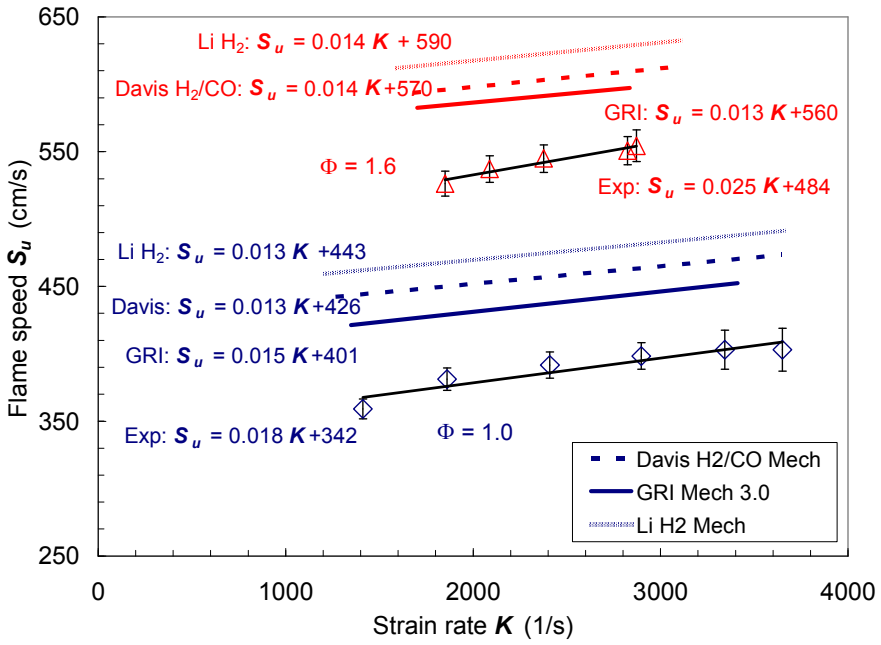

Figure 5. Strained laminar flame speeds for stoichiometric and rich mixtures of H_2 and N_2 diluted air (O_2:N_2 1:9) with 700 K preheat temperature; data (symbols and thin line=linear fit) and OPPDIF predictions (thick lines). Equations of the best-fit lines to the experimental data and the model results are also shown.

Experiments and simulations were also conducted for stoichiometric and rich (Φ=1.6) mixtures of H_2 and N_2 diluted air (Figure 5). As in the lean case, all three models over predict the

measurements. Now however, the model results are closer to one another than to the measurements. The GRI mechanism again has the smallest amount of over prediction (12% at Φ=1.0 and 10% at Φ=1.6), the H_2 mechanism produces the highest flame speeds (over prediction of 22% at Φ=1.0 and 15% at Φ=1.6), and the H_2/CO mechanism is in between (18% high at Φ=1 and 12% at Φ=1.6).

By comparing the results at Φ=0.8, 1.0 and 1.6 (Figure 4 and Figure 5), we find that the difference between the model predictions and the measurements increases (for the N_2 diluted air) as the mixture becomes leaner. It is also interesting to consider the behavior of the strain sensitivity. The measured strain sensitivity varies with equivalence ratio, decreasing from 0.049 cm at Φ=0.8 to 0.018 cm at Φ= 1.0, and then increasing to 0.025 cm as the equivalence ratio increases further to 1.6. By comparison, the strain sensitivities predicted by the models are nearly the same (~0.014-0.015 cm), and despite the significant variation in equivalence ratio, the predicted strain sensitivities change only slightly.

Room temperature reactants

The temperature dependence of the flame speeds can be investigated by comparing the current preheated reactant results to previous data with room temperature reactants. Below, the predicted unstrained laminar flame speeds are compared with the stretch corrected flame speed measurements of Egolfopoulos *et al.*[20] for essentially the same fuel and oxidizer mixtures considered above.

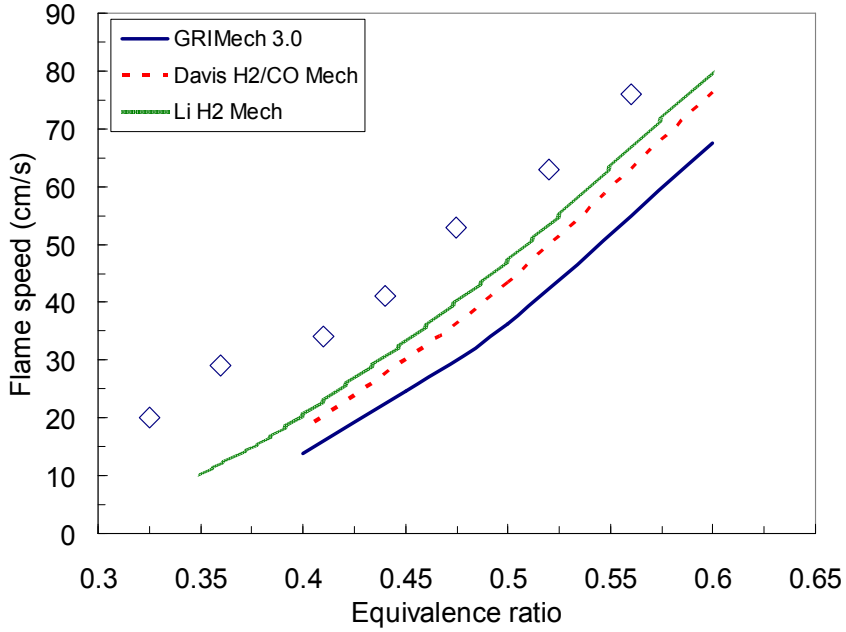

Figure 6. Unstrained laminar flame speeds for lean mixtures of H_2 and standard air at 298 K; data (Egolfopoulos *et al.*[20]) and PREMIX predictions (lines).

H_2 with standard air

The experimental and model results for unstrained laminar flame speed for H_2 and standard air at 298 K are shown in Figure 6 for a range of lean equivalence ratios. As opposed to the corresponding preheat cases (Figure 3), where the models slightly under predict or over predict the experimental data, all three models significantly under predict the experimental results for

low temperature reactants. In addition, the amount of under prediction increases as the mixture becomes leaner.

The H_2 mechanism, which was the farthest from the data at high preheat, now produces results that are closest to the measured room temperature flame speeds (15% too low at Φ=0.5). The GRI mechanism, which produced predictions closest to the high temperature flame speeds, has the greatest discrepancy at room temperature, under predicting the measurements by 35% at Φ=0.5. Thus by comparing the low and high temperature results, we find the models over predict the temperature dependence of the flame speed for H_2-air mixtures under the lean conditions studied.

It is interesting to note that ignition delay studies have also found that the GRI and H_2/CO mechanisms have difficulty matching experimental results at low reactant temperatures for high H_2 content fuels, though they do well at higher temperatures. Specifically the models were found to over predict the ignition delay at ~900 K for lean, atmospheric pressure syngas fuel mixtures with high H_2 content.[21] This is consistent with the under prediction of flame speeds observed in the current study, since longer ignition delays correspond to lower reaction rates.

H_2 with N_2 diluted air

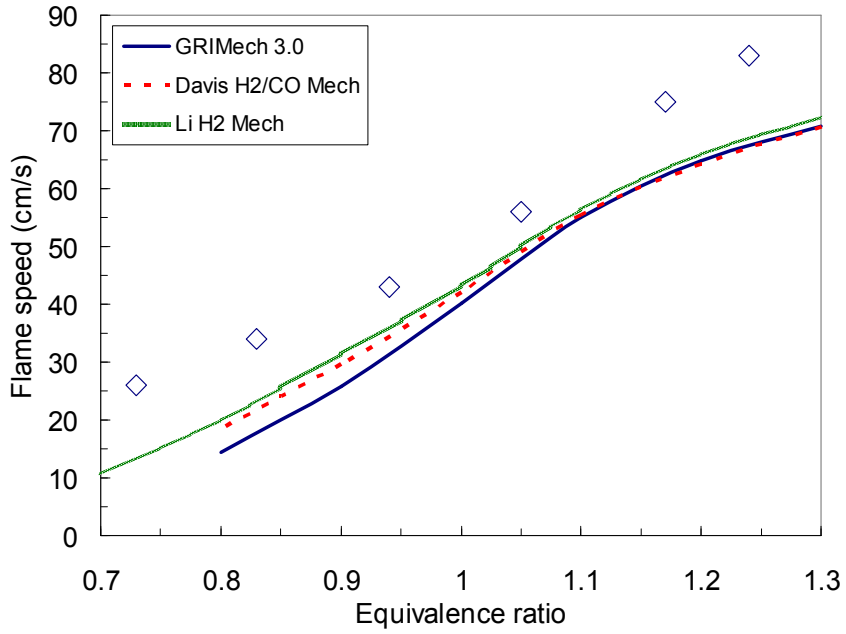

Figure 7. Unstrained laminar flame speeds for H_2 with N_2 diluted air (O_2:N_2 of 1:8.35) mixtures at 298 K; data (Egolfopoulos *et al.*[20]) and PREMIX predictions (lines).

The measured and predicted unstrained laminar flame speeds for H_2 with N_2 diluted air (O_2:N_2 1:8.35) at 298 K are shown in Figure 7 for lean and rich mixtures. As with the undiluted results, all the mechanisms under predict the measurements. By comparison, the model predictions were higher than the measured flame speeds in the highly preheated case. The amount of under prediction increases as mixture moves away from near stoichiometric conditions. For lean mixtures, similar to the undiluted case, the H_2 mechanism is closest to the measurements (within 10% and 30% at Φ=1.0 and 0.8), and the GRI mechanism results are the farthest (15% and 50%

at Φ=1.0 and 0.8). As the mixture becomes fuel rich, all three mechanisms produce essentially the same flame speeds. Comparing the low and high temperature results, we again find that the models predict a higher temperature dependence for the flame speed than is found from the measurements.

5. Summary and Concluding Remarks

The effect of reactant preheating on the laminar flame speeds of H_2 mixed with air and with air highly diluted with N_2 has been investigated. Strained laminar flame speeds and strain sensitivities were measured in a wall stagnation flame with 700 K preheat temperature. The measurements are compared with numerical predictions based on three leading chemical kinetic mechanisms, each with its own thermal and transport property database and each optimized for a different fuel system that includes oxyhydrogen reactions.

For mixtures of H_2 and standard air, both the measured and predicted flame speeds vary linearly with strain. In addition, the modeled flame speeds and their sensitivity to strain are in reasonable agreement with the measurements, at least for the lean conditions studied here. However, the models over predict the measured flame speeds and under predict the strain sensitivities for the highly diluted mixtures. Moreover the amount of flame speed over prediction increases as the mixture becomes more lean, and all three models predict almost no variation in the strain sensitivity with equivalence ratio, in contrast to the experimental results. The results with dilution and lean mixtures are especially relevant to low emissions combustion applications involving syngas fuels that contain significant hydrogen and diluent fractions.

In contrast, comparisons of the model results to previous measurements indicate that all the models significantly under predict the measured flame speeds for room temperature reactants. For example, the model that produces the best results for high preheat temperature (GRIMech 3.0) has the largest discrepancy at low temperature.

We therefore conclude that the temperature dependence of the hydrogen flame speed as predicted by the models is greater than the actual temperature dependence for both standard and diluted air. Since all three models exhibit this same behavior, it is likely that they share a common cause. The source could be an error in the temperature dependence of one or more reaction rates, or in transport properties; this is currently under investigation.

Acknowledgments

The authors would like to acknowledge the support of Siemens Power Generation under a subcontract from the U.S. Department of Energy.

Appendix

Effect of wall boundary conditions

For all the strained flame speed predictions, the Chemkin opposed flow code was used with two premixed flames on either side of the stagnation plane; the simulation is adiabatic. In the experiments, however, a solid wall replaces one of the premixed jets, which makes the system nonadiabatic due to the loss of heat from the product gases to the solid wall. This could potentially reduce the unburned strained flame speeds. Moreover in the opposed flame case, the radial velocity gradient at the stagnation plane is finite (due to a slip condition), while it is zero at the plug wall (due to a no slip condition) for the single jet wall case. This zero radial velocity gradient changes the strain rate distribution in the product zone, which could change the unburned flame speed. In order to investigate the effects of both heat loss and no-slip condition at the wall, a detailed numerical analysis was conducted on a wall stagnation flame configuration, and the results were compared with that of the opposed flame case.

The wall stagnation flame was simulated with the Chemkin opposed flow code, but with modified boundary conditions. For the opposed flow code there are two nozzles separated by distance L. The boundary conditions at each nozzle exit are the same: $T = T_i$, $F = \rho u/2$, $G = \rho v/r$, and for the species, the sum of convection and diffusion is equal to the total inflow mass flux. Here, F and G are the parameters defining axial (u) and radial (v) velocities respectively and they are function of x only. To simulate the wall stagnation flame, one of the nozzle boundary conditions is changed as follows: the axial velocity is zero ($F=0$), the temperature is $T=T_{wall}$, the radial velocity gradient is zero ($G = 0$), and for the species the diffusive velocity is zero. All of these boundary conditions can be applied in the opposed flow code by considering the top nozzle as a solid wall and specifying $u=0$ and $T=T_{wall}$. The other two boundary conditions for the radial velocity gradient and the species are automatically satisfied. The distance between the nozzles has to be reduced from L to $L/2$. Figure 8 shows the variation of the temperature and radial velocity gradient along the axial direction for both opposed flame (OPF) and wall stagnation flame (WSF) for the same mixture, fuel-air ratio and single-jet flowrate. In this example, L=0.6 cm and the axial velocity at the nozzle exit is 1.2 m/s. The temperature of the wall is 900 K (for the wall stagnation flame).

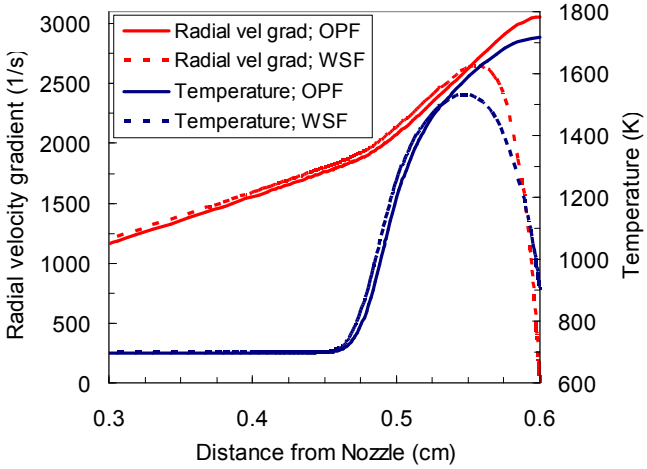

Figure 8. Numerical simulation of opposed flame (OPF) and wall stagnation flame (WSF) for H_2 with N_2 diluted air (O_2:N_2 1:9) at Φ=0.8 and 700 K preheat temperature

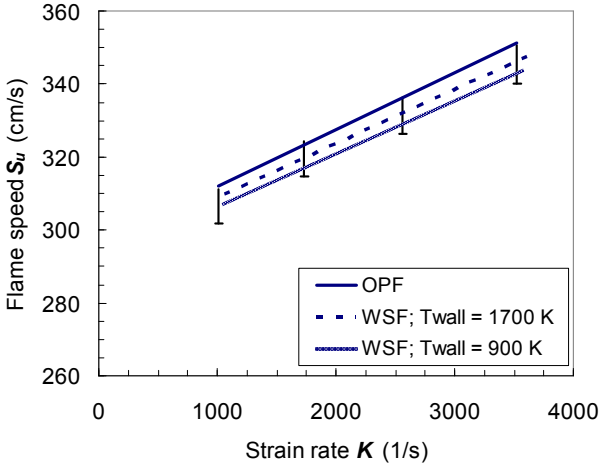

Figure 9. Variation of the strained flame speed for OPF and WSF with two different wall temperatures. The vertical bars indicate 3% deviation from OPF

For both cases, the flame is located ~0.46 cm from the nozzle exit. The temperature for the OPF case increases and reaches a maximum (1717 K) at the stagnation plane. For the WSF case, the temperature rise is nearly identical in the preheat zone, but it reaches a lower maximum (1531 K) somewhere in the reaction zone, afterwards decreasing due to heat loss to the wall (and reaching the specified 900 K at the wall stagnation plane). The radial velocity gradient, in a similar fashion to the temperature, increases and reaches maximum at the stagnation plane for the OPF case. For the WSF case, it increases and then decreases to zero at the wall in order to satisfy the no-slip condition at the stagnation plane. Thus there is a significant change in strain rate distribution in the product zone close to the wall. Moreover the wall stagnation flame is slightly displaced further from the stagnation surface compared to the opposed (twin flame) case.

Numerical simulations of OPF and WSF were carried out for H_2 with N_2 diluted air (O_2:N_2 1:9) at Φ=0.8 and 700 K preheat temperature. This fuel composition is chosen for detailed investigation because it is expected to be more sensitive to heat loss for two reasons: 1) the flame is located closer to the wall (within about two flame thicknesses) compared to the other cases reported here, and 2) the temperature and velocity rise across the (weaker) flame are smaller. Figure 9 shows the strained flame speed predicted with GRI Mech over a range of strain rates for both the OPF and WSF. For the WSF, simulations were performed for two wall temperatures (900 and 1700 K). The heat loss will clearly be very small for T_{wall}=1700 K, because the temperature at the stagnation plane for the OPF case is nearly the same value. Hence the effect of no-slip boundary condition at the wall should dominate for this simulation. For the T_{wall} = 900 K case, however, the amount of heat loss is much greater and hence the effect of both heat loss and no-slip boundary condition can be studied.

The predicted strained flame speed increases linearly for all three cases over the range of strain rates simulated. Moreover the predicted strain sensitivities are almost the same for all three cases. Comparing the strained flame speeds, the WSF predictions are always lower than the OPF predictions. The WSF predictions with T_{wall}=1700 K under predict the OPF by less than 2%. Since the temperatures at the stagnation plane are nearly the same for both cases, the zero radial velocity gradient at the wall is seen to slightly reduce the strained flame speed. When the wall temperature is reduced further, the predicted strained flame speed decreases slightly more. For T_{wall}=900 K, the predicted flame speeds are now below the OPF results by less than 3% throughout the strain rate range tested. Even though the flame (product) temperature is lower for the WSF due to greater downstream heat loss, the unburned strained flame speed is not significantly altered (even when the flame is located within two flame thicknesses from the wall).

Effect of nozzle boundary conditions

The strained flame speeds presented here were calculated using the Chemkin opposed flow code with plug flow boundary conditions at the nozzle exit. Since the experiments employed a high contraction ratio nozzle, the nozzle exit flow should be close to plug flow. However due to non-ideal behavior at the nozzle exit (wall boundary layer and pressure gradient induced by the stagnation condition), the exit velocity profile could slightly deviate from the plug flow boundary condition. This could potentially change the minimum axial velocity (identified as the strained flame speed) between the experiments and simulations for the same imposed strain rate (defined as the maximum gradient in the reactants). For large deviations from plug flow, one would expect the inflow boundary condition to approach a plug flow. Therefore, detailed numerical

simulations were performed for plug and potential flow boundary conditions for the fuel mixtures and experimental conditions (Φ, *L* and strain rates) reported here. Figure 10 shows the variation of the axial velocity for both boundary conditions at identical strain rates. While the flame location for the potential flow is closer to the nozzle than for the plug flow, the minimum velocity before the flame is not affected significantly by the change in boundary condition. The minimum velocity for the potential flow case is 350.7 cm/s, while it is 345.4 cm/s for the plug flow boundary condition (less than a 1.5% effect). Similar analyses were performed for a range of strain rates for mixtures of H_2 with N_2 diluted air at Φ=0.8 and 700 K preheat temperature (Figure 11). The predicted flame speed with potential flow boundary conditions is less than that of the plug flow boundary conditions for all the strain rates, but the difference between the two is within 2%. This indicate that the minimum velocity axial velocity is not very sensitive to the boundary conditions (for the same applied strain rate defined by the maximum velocity gradient ahead of the flame). Hence the small deviations from plug flow that might be expected in the experimental nozzle boundary condition can be neglected (at least for the mixtures tested here).

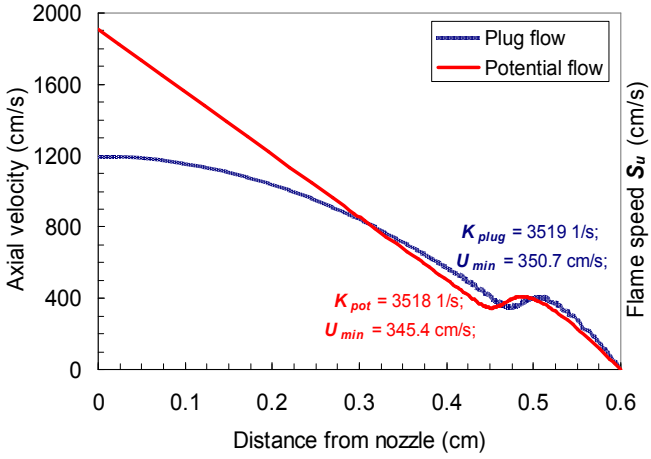

Figure 10. Numerical simulation of plug and potential flow boundary condition for the same strain rates; H_2 with N_2 diluted air (O_2:N_2 1:9) at Φ=0.8 and 700 K preheat temperature.

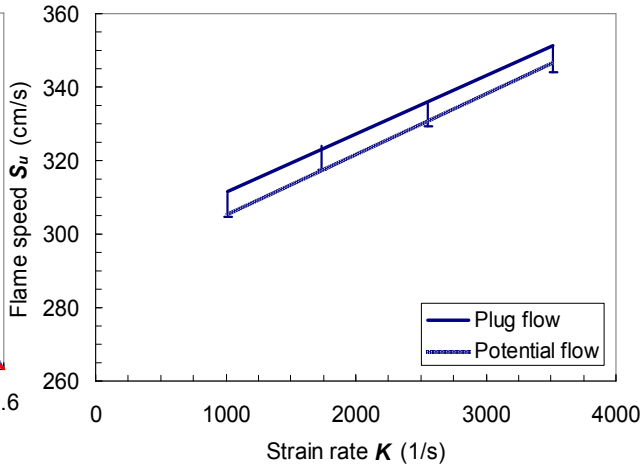

Figure 11. Variation of the strained flame speed for plug and potential flow boundary conditions. The vertical bars indicate 2% deviation.

References

[1] Moliere, M. (2002). "Benefiting from the wide fuel capability of gas turbines: A review of application opportunities." *ASME Paper GT-2002-30017*.

[2] Klimstra, J (1986). "Interchangeability of Gaseous Fuels – The Importance of the Wobbe Index," *SAE Paper 861578*.

[3] Scholte, T. G., and Vaags, P. B. (1959). "Burning velocities of mixtures of hydrogen, carbon monoxide, and methane with air." *Combustion and Flame* **3**, 511-524.

[4] Strauss, W. A., and Edse, R. (1958). "Burning velocity measurements by the constant-pressure bomb method." *Proceedings of the Combustion Institute* **7**: 377-385.

[5] Yumlu, V. S. (1967). "Prediction of burning velocities of carbon monoxide-hydrogen-air flames." *Combustion and Flame* **11**: 190-194.

[6] Vagelopoulos, C. M., and Egolfopoulos, F. N. (1994). "Laminar flame speeds and extinction strain rates of mixtures of carbon monoxide with hydrogen, methane, and air." *Proceedings of the Combustion Institute* **25**: 1317-1323.

[7] McLean, I. C., Smith, D. B., and Taylor, S. C. (1994). "The use of carbon monoxide/hydrogen burning velocities to examine the rate of the CO + OH reaction." *Proceedings of the Combustion Institute* **25**: 749-757.

[8] Brown, M. J., McLean, I. C., Smith, D. B., and Taylor, S. C. (1996). "Markstein lengths of CO/H_2/air flames, using expanding spherical flames." *Proceedings of the Combustion Institute* **26**: 875-881.

[9] Hassan, M. I., Aung, K. T., and Faeth, G. M. (1996). "Markstein numbers and unstretched laminar burning velocities of wet carbon monoxide flames." *AIAA 96-0912*, *34th Aerospace Sciences Meeting & Exhibit, Reno, NV*.

[10] Hassan, M. I., Aung, K. T., and Faeth, G. M. (1997). "Properties of laminar premixed CO/H_2/air flames at various pressures." *Journal of Propulsion and Power* **13**(2): 239-245.

[11] Davis, S. G., Joshi, A. V., Wang, H., and Egolfopoulos, F. N. (2004). "An optimized kinetic model of H_2/CO combustion" *Proceedings of the Combustion Institute* **30**. 1283-1292.

[12] Li, J., Zhao, Z., Kazakov, A., Chaos, M., Dryer, F. L., and Scire Jr, J. J. (2007). "A Comprehensive kinetic mechanism for CO, CH2O, and CH3OH combustion." *Int. J. Chem. Kin.*

[13] Natarajan, J., Nandula, S., Lieuwen, T., and Seitzman, J. (2005). "Laminar Flame Speeds of Synthetic Gas Fuel Mixtures." *ASME Paper GT-2005-68917*.

[14] Wu, C. K., and Law, C. K. (1984). "On the determination of laminar flame speeds from stretched flames." *Proceedings of the Combustion Institute* **20**: 1941-1949.

[15] Vagelopoulos, C. M., Egolfopoulos, F. N., and Law, C. K. (1994). "Further considerations on the determination of laminar flame speeds with the counterflow twin-flame technique." *Proceedings of the Combustion Institute* **25**: 1341-1347.

[16] Egolfopoulos, F. N., Zhang, H., and Zhang, Z. (1997). "Wall effects on the propagation and extinction of steady, strained, laminar premixed flames." *Combustion and Flame* **109**, 237-252.

[17] Andac, M. G., Egolfopoulos, F. N., and Campbell, C. S. (2002). "Premixed flame extinction by inert particles in normal and micro-gravity." *Combustion and Flame* **129**, 179-191.

[18] Smith, G. P., Golden, D. M., Frenklach, M., Moriarty, N. W., Eiteneer, B., Goldenberg, M., Bowman, C. T., Hanson, R. K., Song, S., Jr Gardiner, W. C., Lissianski, V. V., and Qin, Z. http://www.me.berkeley.edu/gri_mech/

[19] Li, J., Zhao, Z., Kazakov, A., and Dryer, F. L., (2004) "An updated comprehensive kinetic model of hydrogen combustion" *Int. J. Chem. Kin.* **36** 566-575.

[20] Egolfopoulos, F. N., and Law, C. K. (1990). "An experimental and computational study of the burning rates of ultra-lean to moderately-rich $H_2/O_2/N_2$ laminar flames with pressure variation" *Proceedings of the Combustion Institute* **23**: 333-340.

[21] Kalitan, D. M., and Peterson, E. L. (2005). "Ignition and oxidation of lean CO/H_2 fuel belnds in air" *41st AIAA/ASME/SAE/ASEE Joint Propulsion Conference & Exhibit, Tucson, Arizona*.